

Antimicrobial coatings based on zinc oxide and orange oil for improved bioactive wound dressings and other applications

MARIUS RĂDULESCU¹⁾, ECATERINA ANDRONESCU²⁾, ANDREEA CÎRJA²⁾, ALINA MARIA HOLBAN²⁻⁴⁾, LAURENȚIU MOGOANTĂ⁵⁾, TUDOR-ADRIAN BĂLȘEANU⁶⁾, BOGDAN CĂTĂLIN⁶⁾, TIBERIU PAUL NEAGU⁷⁾, IOAN LASCĂR⁷⁾, DENISA ALEXANDRA FLOREA⁸⁾, ALEXANDRU MIHAI GRUMEZESCU²⁾, BIANCA CIUBUCA^{3,4)}, VERONICA LAZĂR^{3,4)}, MARIANA CARMEN CHIFIRIUC^{3,4)}, ALEXANDRA BOLOCAN⁹⁾

¹⁾Department of Inorganic Chemistry, Physical Chemistry and Electrochemistry, Faculty of Applied Chemistry and Materials Science, University Politehnica of Bucharest, Romania

²⁾Department of Science and Engineering of Oxide Materials and Nanomaterials, Faculty of Applied Chemistry and Materials Science, University Politehnica of Bucharest, Romania

³⁾Department of Microbiology–Immunology, Faculty of Biology, University of Bucharest, Romania

⁴⁾Division of Earth, Environmental and Life Sciences, Research Institute of the University of Bucharest (ICUB), Bucharest, Romania

⁵⁾Research Center for Microscopic Morphology and Immunology, University of Medicine and Pharmacy of Craiova, Romania

⁶⁾Research Center for Clinical and Experimental Medicine, University of Medicine and Pharmacy of Craiova, Romania

⁷⁾Department of Plastic Surgery and Reconstructive Microsurgery, "Carol Davila" University of Medicine and Pharmacy, Bucharest, Romania

⁸⁾Department of Biomaterials and Medical Devices, Faculty of Medical Engineering, University Politehnica of Bucharest, Romania

⁹⁾Emergency University Hospital, Bucharest, Romania; "Carol Davila" University of Medicine and Pharmacy, Bucharest, Romania

Abstract

This work presents a novel nano-modified coating for wound dressings and other medical devices with anti-infective properties, based on functionalized zinc oxide nanostructures and orange oil (ZnO@OO). The obtained nanosurfaces were characterized by transmission electron microscopy (TEM), scanning electron microscopy (SEM), selected area electron diffraction (SAED), differential thermal analysis–thermogravimetry (DTA–TG), X-ray diffraction (XRD), and Fourier transform infrared (FT-IR) spectroscopy. The obtained nanocomposite coatings exhibited an antimicrobial activity superior to bare ZnO nanoparticles (NPs) and to the control antibiotic against *Staphylococcus aureus* and *Escherichia coli*, as revealed by the lower minimal inhibitory concentration values. For the quantitative measurement of biofilm-embedded microbial cells, a culture-based, viable cell count method was used. The coated wound dressings proved to be more resistant to *S. aureus* microbial colonization and biofilm formation compared to the uncoated controls. These results, correlated with the good *in vivo* biodistribution open new directions for the design of nanostructured bioactive coating and surfaces, which can find applications in the medical field, for obtaining improved bioactive wound dressings and prosthetic devices, but also in food packaging and cosmetic industry.

Keywords: zinc oxide, nanoparticles, orange essential oil, antimicrobial, antibiofilm, modified wound dressing.

Introduction

Zinc oxide (ZnO) is widely used in various applications in different fields, including the biomedical one, primarily due to its well-established antimicrobial activity [1–3]. Also, some studies underline the contribution of ZnO to improved wound healing and higher epithelialization rates. These effects could be explained by the fact that zinc represents a co-factor of different transcription factors and zinc-dependent enzymes involved in wound repair. Its efficiency has been demonstrated particularly after topic administration, by reducing infections and local inflammation and stimulating epithelialization [4, 5]. An immunomodulatory effect has been shown for sub-toxic concentrations of ZnO in nanosized form [6, 7]. These effects motivated the development of different dressings containing ZnO as an active component. ZnO can be

coated on different wound dressings in order to improve their antimicrobial and wound pro-healing effect [8]. Plant extracts have been used for thousands of years around the world, as traditional treatments for many diseases and currently, approximately 80% of the population of developing countries still uses traditional medicine for the treatment of a wide range of diseases [9]. Essential oils are mixtures of various chemical constituents resulted in plant secondary metabolism with different therapeutic properties. The therapeutic properties of these extracts include anti-infective, antioxidant and immunomodulatory actions, which could be of benefit for the wound healing process. There are several studies that document the use of plant extracts in the development of bioactive wound dressings [10].

The purpose of the current paper was to obtain and characterize the physico-chemical and biological activities

of novel nano-modified coating for wound dressings and other medical devices with anti-infective properties, based on functionalized ZnO nanostructures and orange oil.

☞ Materials and Methods

Materials

All chemicals used in the experiments were of analytical reagent grade and were used without further purification.

Preparation of modified wound dressing

Zinc oxide nanoparticles were prepared according to our previously study with slight modification [11]. Two solutions were prepared as follow: (i) 100 mL solution of $\text{Zn}(\text{NO}_3)_2 \cdot 6\text{H}_2\text{O}$ (3%) and (ii) 100 mL solution of NaOH (3%) that contain 500 μL orange oil (OO). These solutions were vigorously stirred and the aqueous basic solution of OO was added drop by drop into the zinc solution. This obtained dispersion was filtered several times in order to remove the secondary products and excess of OO.

Modified wound dressing was prepared in the same way. In the solution containing sodium hydroxide and OO there were added wound dressings (aseptically cut in samples of 1 cm^2) and then, $\text{Zn}(\text{NO}_3)_2 \cdot 6\text{H}_2\text{O}$ solution was added drop by drop. After the precipitation of ZnO nanoparticles on the surface of wound dressing samples, the modified wound dressings were washed several times with distilled water and dried at room temperature until further processing and characterization.

Characterization methods

X-ray diffraction (XRD)

XRD analysis was performed on a Shimadzu XRD 6000 diffractometer at room temperature. In all the cases, Cu $K\alpha$ radiation from a Cu X-ray tube (run at 15 mA and 30 kV) was used. The samples were scanned in the Bragg–Brentano geometry with 2θ angle range of 20–80°.

Scanning electron microscopy (SEM)

SEM analysis was performed on a FEI electron microscope, using secondary electron beams with energies of 30 keV, on samples covered with a thin gold layer.

Infrared (IR) analysis

IR mappings were recorded on a Nicolet iN10 MX FT-IR (Fourier transform infrared) microscope with MCT (Hg–Cd–Te) liquid nitrogen cooled detector in the measurement range 4000–700 cm^{-1} . Spectral collection was made in reflection mode at 4 cm^{-1} resolution. For each spectrum, 32 scans were co-added and converted to absorbance using OmnicPicta software (Thermo Scientific). Approximately 250 spectra were analyzed for each sample. One absorption peak known as being characteristics for the prepared material was selected as spectral marker.

Thermogravimetry (TG)

TG analysis of the biocomposite was assessed with a Shimadzu DTG-TA-50H instrument. Samples were screened to 200 mesh prior to analysis, were placed in alumina crucible, and heated with 10 K/min. from room

temperature to 800°C, under the flow of 20 mL/min. dried synthetic air (80% N_2 and 20% O_2).

Transmission electron microscopy (TEM)

TEM images were obtained on finely powdered samples using a Tecnai™ G2 F30 S-TWIN high-resolution transmission electron microscope from FEI Company (Hillsboro, OR, USA) equipped with selected area electron diffraction (SAED). The microscope operated in transmission mode at 300 kV with TEM point resolution of 2 Å and line resolution of 1 Å. The microspheres were dispersed into pure ethanol and ultrasonicated for 15 minutes. After that, diluted sample was poured onto a holey carbon-coated copper grid and left to dry before TEM analysis.

In vivo biodistribution study

The experimental protocol was applied according with the European Council Directive No. 86/609/24 November 1986, the European Convention on the Protection of Vertebrate Animals (2005) and the Romanian Government Ordinance No. 37/2 February 2002. The mice organs were collected under general anesthesia. Biological material was fixed, directly after the sampling, in 10% buffered neutral formalin, for 72 hours, at room temperature, and then processed for routinely histological paraffin embedding technique. For the histological study of nanoparticles, 4 μm thick serial sections were cut on a MICROM HM355s rotary microtome (MICROM International GmbH, Walldorf, Germany) equipped with a waterfall-based section transfer system (STS, MICROM). The cross-sections were placed on histological blades treated with poly-L-Lysine (Sigma-Aldrich, Munich, Germany). After Hematoxylin–Eosin (HE) classical staining, cross-sections were evaluated and photographed using a Nikon Eclipse 55i light microscope equipped with a Nikon DS-Fi1 CCD high-definition video camera (Nikon Instruments, Apidrag, Bucharest, Romania). Images were captured, stored and analyzed using Image ProPlus 7 AMS software (Media Cybernetics Inc., Marlow, Buckinghamshire, UK) [12, 13].

Minimal inhibitory concentration (MIC) assay

The antimicrobial activity of the obtained nanocomposite suspensions was assayed on Gram-negative (*Escherichia coli* ATCC 13202) and Gram-positive (*Staphylococcus aureus* ATCC 6538) reference strains obtained from the American Type Culture Collection (ATCC, Manassas, VA, USA). Microbial suspensions of 1.5×10^8 CFU/mL (0.5 McFarland density) obtained from 15 to 18 hours bacterial cultures developed on solid media were used in our experiments. The nanocomposite suspensions were suspended in dimethyl sulfoxide (DMSO) to prepare a stock solution of 1 mg/mL concentration. The quantitative assay of the antimicrobial activity was performed by the liquid medium microdilution method in 96 multi-well plates. Two-fold serial dilutions of the compounds solutions were performed in a 200- μL volume of broth, and each was well seeded with a volume of 50 μL of microbial inoculum. Culture positive controls (wells containing culture medium seeded with the microbial inoculum) were used. The influence of the DMSO solvent was also quantified in a series of wells containing DMSO, diluted accordingly with the dilution scheme used for the

complexes. The plates were incubated for 24 hours at 37°C, and the minimal inhibitory concentration (MIC) values were considered as the lowest concentration of the tested compound that inhibited the growth of the microbial overnight cultures, as compared to the positive control.

Biofilm assay

For assessing monospecific *S. aureus* biofilm formation, 2 mL of nutritive broth were disposed in each well of a 6-wells plate, containing test (modified dressings) and control (unmodified dressings) samples and seeded with the bacterial inoculum consisting of a volume of 20 µL from the phosphate-buffered saline (PBS) bacterial suspension. After a period of 24 hours incubation at 37°C, the materials containing the attached bacteria were washed with PBS and transferred in a fresh well, containing 2 mL sterile nutritive broth and the incubation continued for another 24 hours. The same procedure was repeated at 48 and 72 hours, in order to assess the biofilm formation on the materials at different time intervals (24, 48 and 72 hours). After each interval, the viable cell count (VCC) method was performed. For this, after each time point, biofilm-embedded bacteria cells were detached by vigorous vortexing for 30 seconds. PBS suspensions containing detached bacteria cells were subjected to serial 10-fold dilutions and each dilution was seeded on nutritive agar in triplicates.

Results

In Figure 1, there are presented the results of the SEM analysis. The ZnO@OO powder is composed of nanometric particles of uniform shape, with an average size of ~20 nm. Some particles are grouped in agglomerates.

From the selected area diffraction pattern obtained on ZnO@OO nanopowders (Figure 2a), we can state that the only crystalline phase identified is the hexagonal form of ZnO [ASTM 80-0075]. Moreover, the SAED images confirm the Miller indices of characteristic crystalline structures identified by XRD. The TEM bright field images (Figure 2, b and c), obtained on ZnO@OO reveals that the powder is composed of polyhedral shaped particles, with an average particle size of approximately 20 nm. By correlating the TEM and the XRD information, as crystallite size is half of the nanoparticles size, we can conclude that every nanoparticle is composed of two crystallites. The nanopowder presents a low tendency to form soft agglomerates. Additional information about the structures of the nanoparticles was found through detailed analysis with HRTEM.

The high-resolution transmission electron microscopy (HRTEM) image (Figure 2d) shows clear lattice fringes of interplanar distances of $d=2.60$ Å for nanocrystalline ZnO, corresponding to Miller indices of (0 0 2) crystallographic planes of hexagonal ZnO. In addition, the regular succession of the atomic planes indicates that the nanocrystallites are structurally uniform and crystalline, with almost no amorphous phase present.

The thermal analysis of ZnO and ZnO@OO nanopowders (Figure 3) are similar up to 150°C. The samples present a mass loss of ~1.75%, corresponding to the residual surface water molecules. Between 150–1000°C

the curves are slightly differentiated, the mass loss of the ZnO@OO sample being higher (6.45% vs. 5.71% for the simple ZnO). This difference can be attributed to the decomposition (evaporation) of the OO that was trapped on the surface of the ZnO nanoparticles. From these values, we estimate that a quantity of 0.7% OO (wt.) was deposited on ZnO surface. The bulk of the mass loss indicated by the thermal analysis corresponds to the elimination of the water and HO⁻ moieties that were bounded on the ZnO nanoparticles surface.

The ZnO@OO nanopowders were investigated by X-ray diffraction. The XRD pattern from Figure 4 has indicated the formation of single-phase compound. The pattern can be indexed to a hexagonal wurtzite structure. The crystallite size of the samples can be estimated from the Scherrer equation, $D=(0.89\times\lambda)/(\beta\times\cos\theta)$, where D is the average grain size, λ is the X-ray wavelength (0.15405 nm), θ and β are the diffraction angle and full width at half maximum (FWHM) of an observed peak, respectively. The strongest peak (1 0 1) at $2\theta=36.24^\circ$ was used to calculate the average crystallite size (D) of ZnO particles. The estimated average crystallite size was 10 nm. It is important to notice that the OO coating and incorporation process does not lead to a change in the structural or chemical properties of the nanocrystalline ZnO phase. The XRD pattern of the ZnO@OO sample shows that the crystalline structure of the ZnO is preserved after the incorporation of the nanoparticles in the essential oil (OO).

Figure 5 shows the adherence of ZnO@OO layer on the substrate, which seems to be very good. On bigger magnification, the aggregates of ZnO particles are clearly seen.

The *in vivo* biodistribution analysis revealed that after two days post-injection, the ZnO@OO nanostructures are absent in the brain, myocardium, kidney and pancreas, but present in small amounts in liver and in relatively high amounts in lung and spleen tissue sections. In the lungs, the nanoparticles were found mainly in/around perivascular macrophages, but also in the interalveolar septa. The nanoparticles were also found in the intravascular cells of the monocyte-macrophage system. The results suggest that monocytes are able to engulf the nanostructures, explaining the presence of nanoparticles in the vascular lumen, both inside but also outside the cells, and possibly in platelets. In the spleen, the distribution of nanoparticles was different between white and red pulp. Nanoparticles preferentially formed aggregates in the red pulp, in the macrophage from the Billroth cordons and sinusoidal capillaries. Although not observed within the white pulp, this area revealed hypertrophy, probably due to the nanoparticles stimulation of the macrophages with multilobular nucleus. The nanoparticles formed brown-blackish, granular, spherical structures, varying in size, with a diameter of up to 2 µm in the spleen and up to 3–4 µm in the lung sections (Figure 6).

Ten days after injection, the nanoparticles were absent in most of the sampled organs, aggregates being visible in low amounts only in the spleen, around and in the macrophages of the red pulp, but in a lower concentration, as compared with the amount observed after two days post-treatment (Figure 7).

The antimicrobial efficiency of the obtained nanobio-composite containing ZnO NPs and orange oil (ZnO@OO)

was compared to that of ZnO NPs and Chloramphenicol, a large spectrum antimicrobial agent currently used for topic applications (Figure 8). The obtained results have shown that ZnO NPs and orange oil exhibit a synergic antimicrobial activity against both microbial strains, as revealed by the lower MIC value of the nanobiocomposite as compared to bare ZnO NPs. The efficiency of the obtained nanocomposite was higher against the *S. aureus* strain, the MIC value being much lower than that of Chloramphenicol (Figure 8).

Taking into account the excellent results obtained for the *S. aureus* strain in planktonic state, we have tested further the anti-biofilm efficiency of the obtained nanocomposite as coating for textile wound dressings. The obtained results have shown that the coated wound dressings are much more resistant to microbial colonization and further biofilm development, as revealed by the decreased number of biofilm-embedded *S. aureus* viable cells, by 3 to 5 logs, after 34, 48 and 72 hours of incubation (Figure 9).

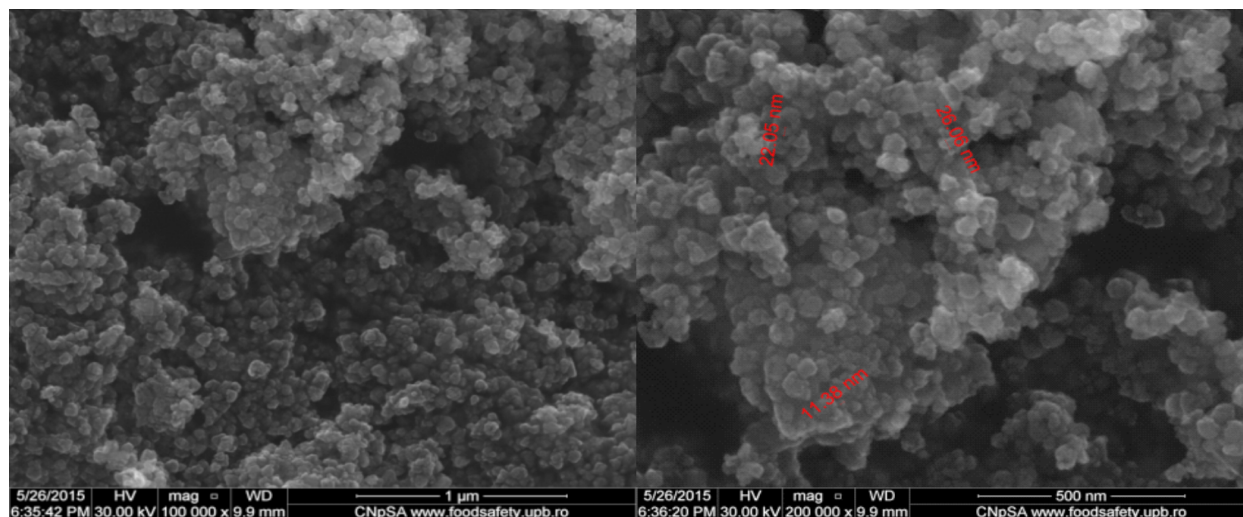


Figure 1 – SEM images of ZnO@OO NPs powder.

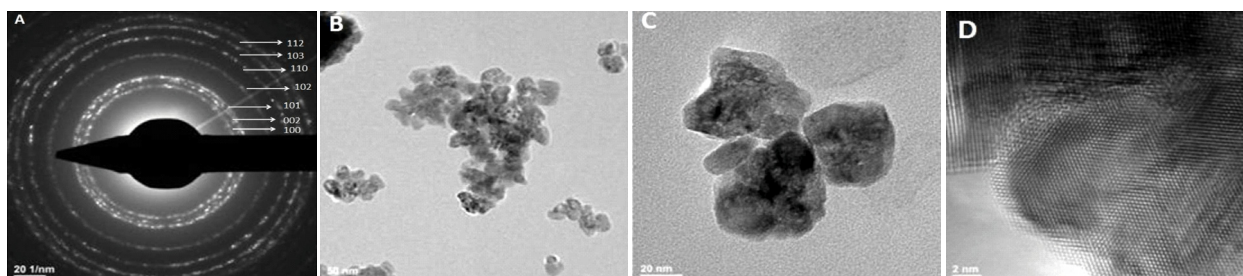


Figure 2 – SAED pattern (A), TEM (B and C) and HRTEM (D) images of ZnO@OO NPs.

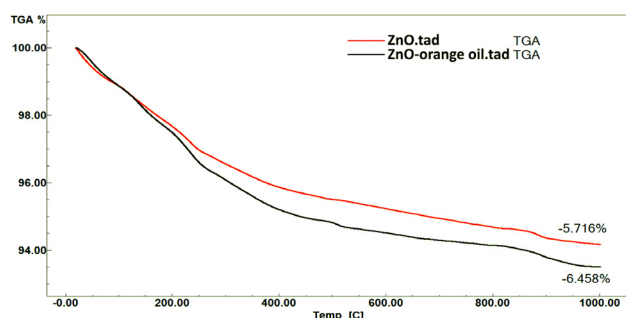


Figure 3 – TG analysis of ZnO and ZnO@OO NPs.

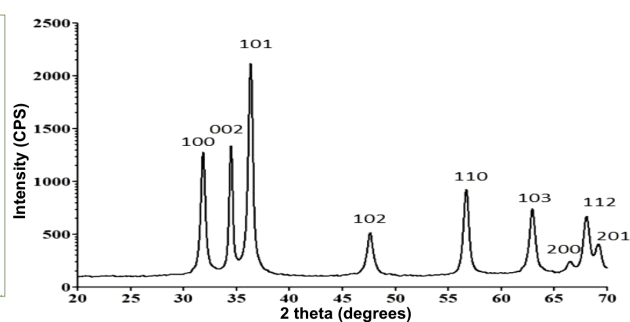


Figure 4 – The XRD pattern of ZnO@OO NPs.

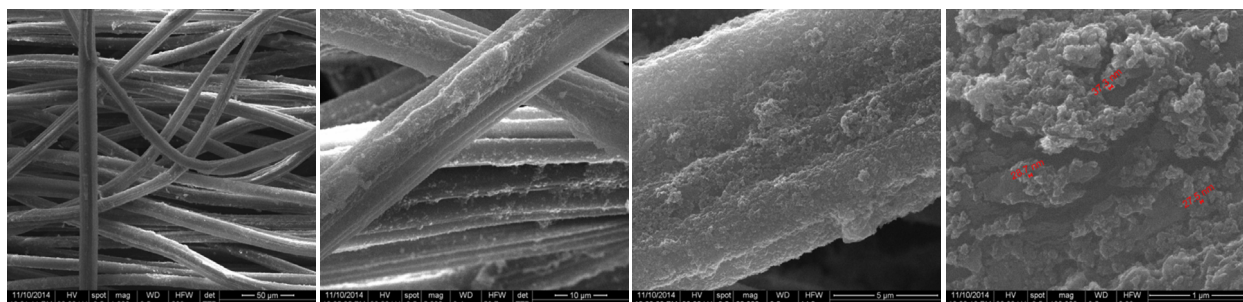


Figure 5 – SEM images of coated wound dressing.

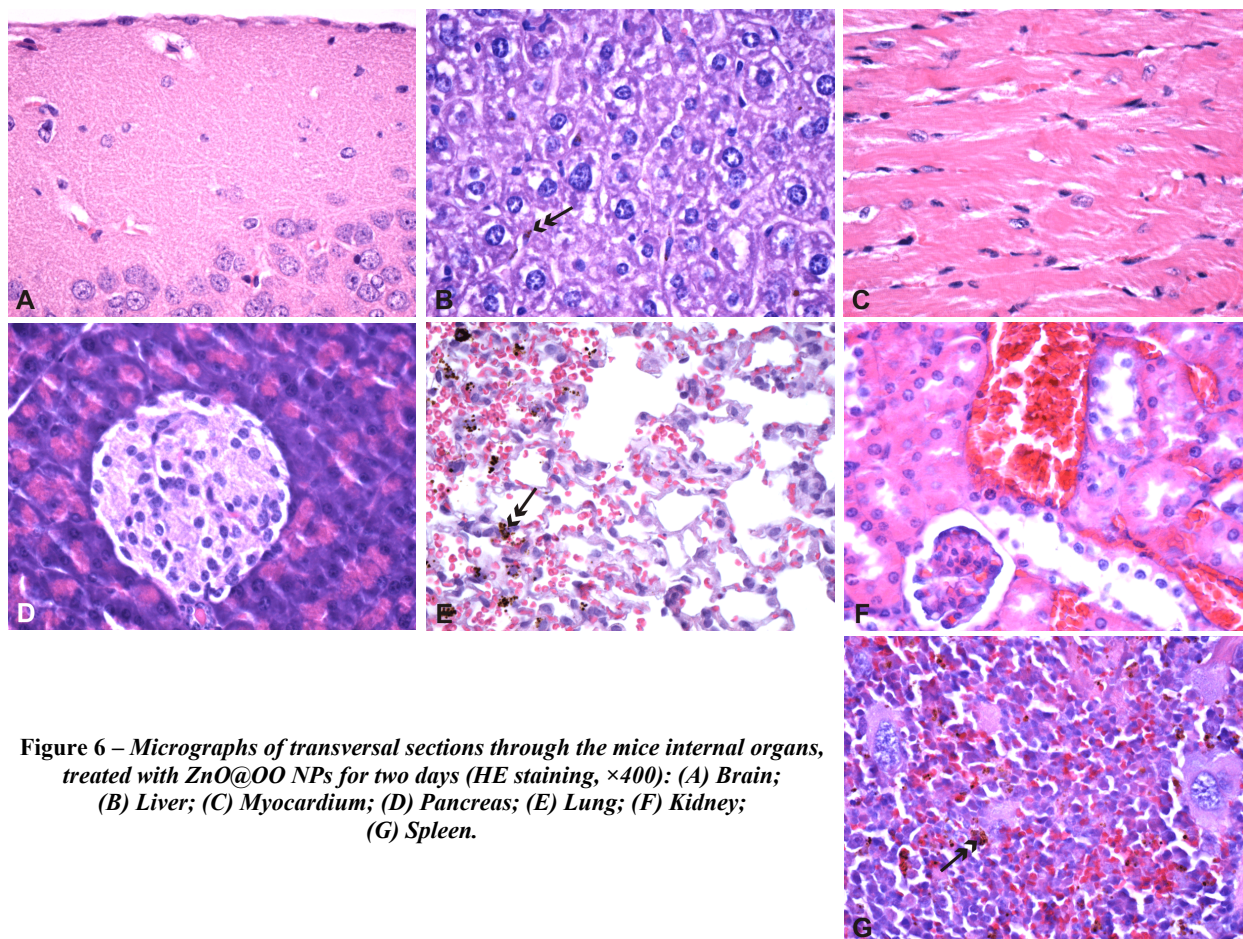


Figure 6 – Micrographs of transversal sections through the mice internal organs, treated with ZnO@OO NPs for two days (HE staining, ×400): (A) Brain; (B) Liver; (C) Myocardium; (D) Pancreas; (E) Lung; (F) Kidney; (G) Spleen.

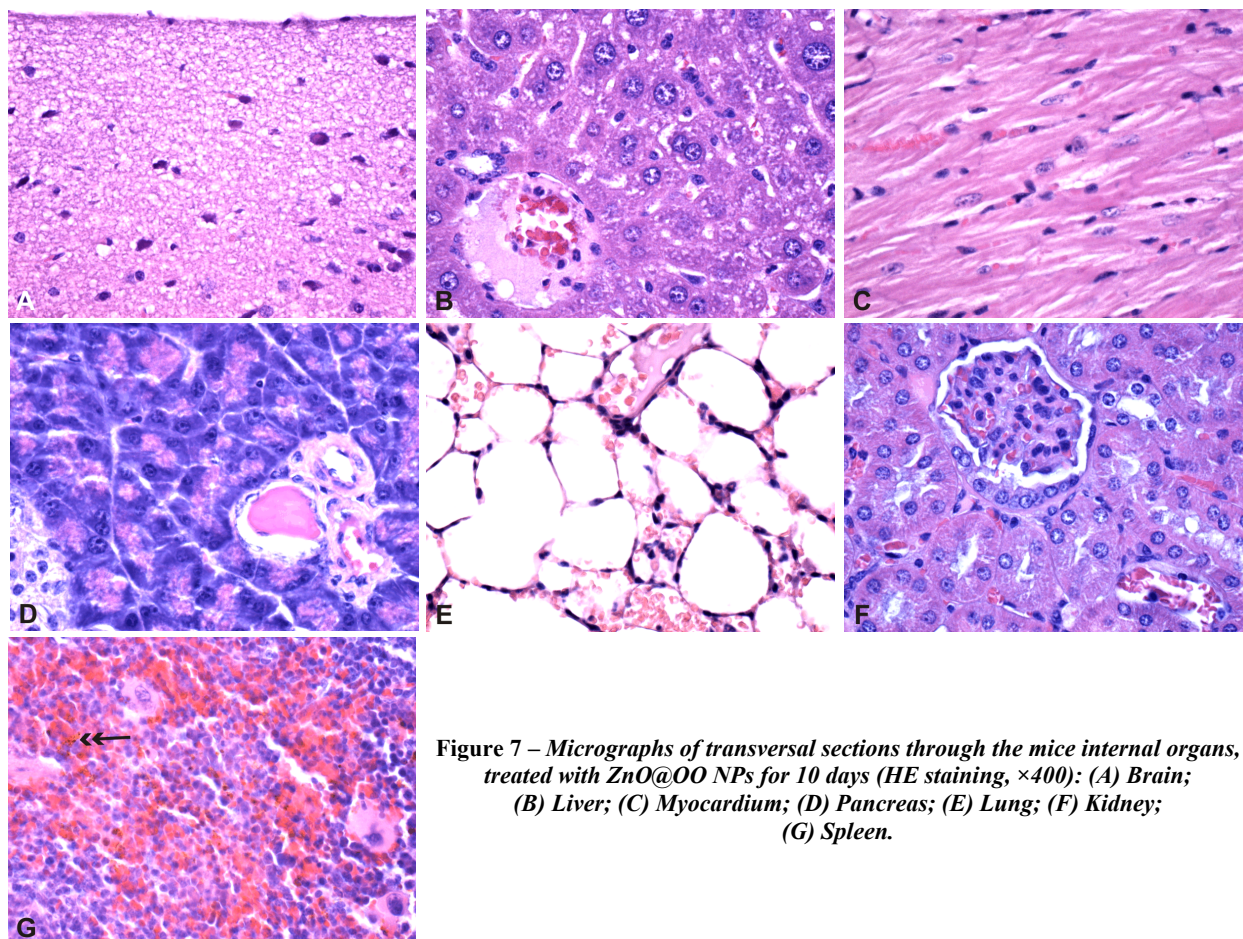


Figure 7 – Micrographs of transversal sections through the mice internal organs, treated with ZnO@OO NPs for 10 days (HE staining, ×400): (A) Brain; (B) Liver; (C) Myocardium; (D) Pancreas; (E) Lung; (F) Kidney; (G) Spleen.

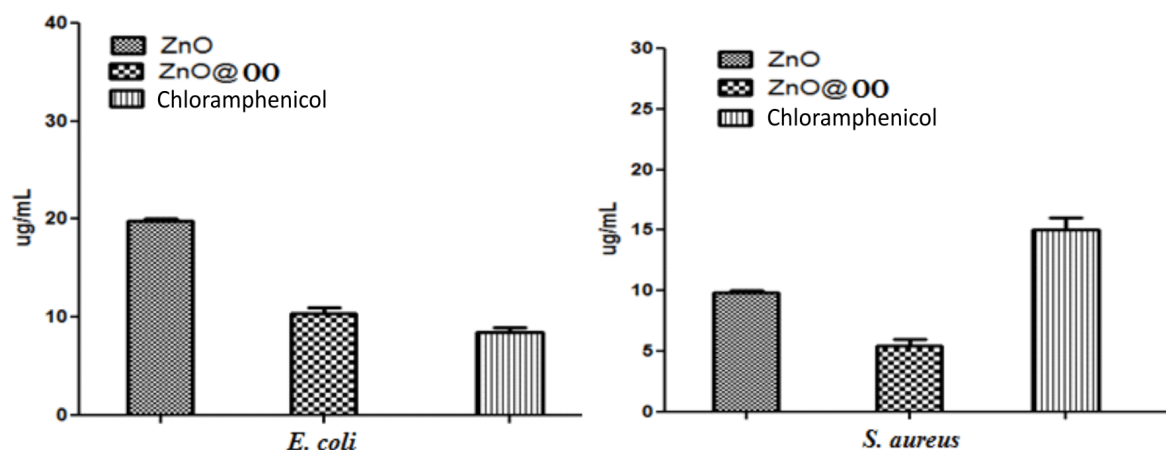


Figure 8 – MIC values of ZnO@OO NPs against *E. coli* and *S. aureus* strains, in comparison with ZnO NPs and Chloramphenicol.

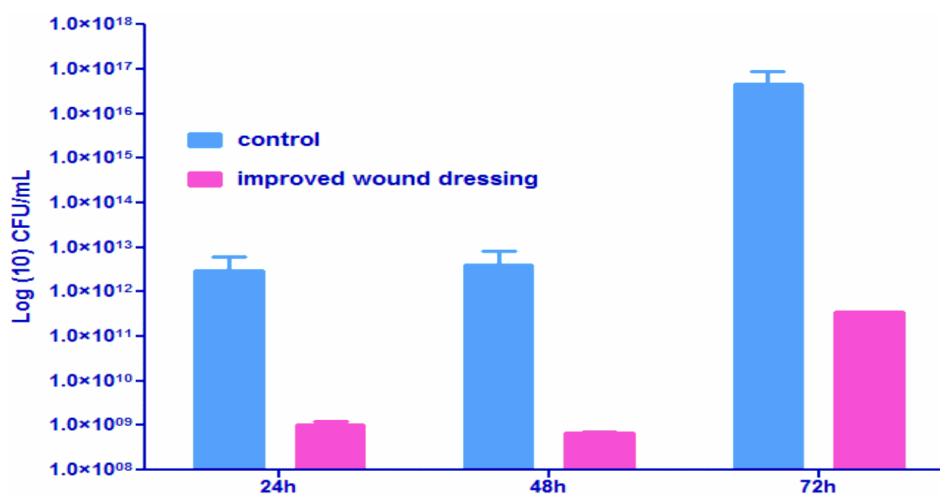


Figure 9 – Graphic representation of the *S. aureus* biofilm formation dynamics on uncoated and coated wound dressings.

Discussion

Wound healing is a complex process depending on both pathophysiological host factors and microbial colonizers. Microbial contamination of acute and chronic wounds is almost inevitable and provides a high risk of wound infection. In order to minimize this risk, the developing of improved dressings and of alternatives to antibiotics to control wound microbiota are needed [14, 15].

ZnO nanoparticles have been shown to exhibit a large spectrum of antimicrobial activity, against Gram-positive and Gram-negative bacteria (e.g., *S. aureus*, *Bacillus subtilis*, *E. coli*, *Pseudomonas fluorescens*, *Salmonella typhimurium*, *Campylobacter jejuni*), halophilic bacteria, yeasts, molds, even against high-temperature and high-pressure resistant endospores, the major mechanisms of action being based on the electrostatic interactions with the negatively charged components of the bacterial wall leading to permeability defects followed by cellular lysis; the production of hydrogen peroxide, enhanced by UV light; the inactivation of intracellular targets [1–3, 16–18]. Among the advantages of using ZnO NPs are the low cost production, white color and the UV barrier properties [1–3]. Essential oils have been traditionally used for the treatment of injured tissues, due to their antimicrobial, anti-inflammatory and tissue pro-healing activity [10, 19,

20]. A modified rayon/polyester wound dressing coated with a nanostructured coating based on functionalized magnetite nanoparticles and *Anethum graveolens*, *Salvia officinalis* and *Satureja hortensis* essential oils proved to be refractory to *Candida albicans* adhesion, colonization and biofilm formation [21, 22]. Modification of absorbent dressings with mixtures of four essential oils proved to efficiently absorb bacterial and fungal strains and limit their growth [23].

The *Melaleuca alternifolia* (tea tree) essential oil included in dressings proved to decrease the wound healing time in volunteer patients who had wounds infected with *S. aureus* [24]. Moreover, recent studies have shown that ratite oil has an accelerating effect on the growth rate of immortalized human keratinocytes and anti-inflammatory properties, which recommend it as a useful component in bandages and ointments for the treatment of wounds and inflammatory skin conditions [25]. *Citrus* plants produce essential oils with antimicrobial properties, devoted to volatile organic compounds, such as β -pinene, sabinene, linalool, *R*-limonene, myrcene, terpineol, geranial (citral), geraniol, linalyl acetate, etc. [26]. In the present study, we have investigated the antimicrobial activity of a novel nanostructure based on ZnO NPs and orange oil against planktonic and biofilm embedded cells. It is well known that biofilm-embedded cells are protected by an extra-

cellular matrix against a wide range of limiting factors, which, at the same time, provides a higher concentration of nutrients [27–31]. The phenotypic resistance of biofilms to antimicrobial factors is rendering the antibiotic regimens inefficient, while simultaneously enabling continuous spreading of biofilm cells [32].

The minimal inhibitory concentration (MIC) value was assessed by the broth microdilution method, against *S. aureus*, as a representative species for the infections with Gram-positive cocci and *E. coli*, as a representative microorganism for the Gram-negative bacterial pathogens. Our results revealed the efficiency of the obtained nanostructures against both planktonic and adherent bacteria, the effect being more intense against the Gram-positive *S. aureus* strain. These results are remarkable, taking into account that this pathogen is the most frequently isolated in chronic wounds infections (diabetic foot ulcers, venous stasis ulcers and pressure sores) associated with biofilm development, being responsible of delays in re-epithelialization and healing going to a two-fold increase in the healing time [33–35].

Conclusions

The obtained nanoparticles exhibited a very good antibacterial activity, both against Gram-positive and Gram-negative strains, while the coated wound dressings proved to be more resistant to *S. aureus* microbial colonization and biofilm formation compared to the uncoated controls. These results correlated with the good *in vivo* biodistribution open new directions for the design of nanostructured bioactive coating and surfaces, which can find applications in the medical field, for obtaining improved bioactive wound dressings and prosthetic devices, but also in food packaging and cosmetic industry.

Conflict of interests

The authors declare no conflict of interests.

Acknowledgments

This work was supported by a grant of the Romanian National Authority for Scientific Research and Innovation, CNCS–UEFISCDI, project number PN-II-RU-TE-2014-4-2269. The SEM analyses on samples were possible due to EU-funding grant POSCCE-A2-O2.2.1-2013-1/Priority direction 2, Project No. 638/12.03.2014, code SMIS-CSNR 48652.

References

- [1] Petrochenko PE, Skoog SA, Zhang Q, Comstock DJ, Elam JW, Goering PL, Narayan RJ. Cytotoxicity of cultured macrophages exposed to antimicrobial zinc oxide (ZnO) coatings on nanoporous aluminum oxide membranes. *Biomater*, 2013 Jul–Sep, 3(3).
- [2] Patrinoiu G, Calderón-Moreno JM, Chifiriuc CM, Saviuc C, Birjega R, Carp O. Tunable ZnO spheres with high anti-biofilm and antibacterial activity via a simple green hydrothermal route. *J Colloid Interface Sci*, 2016, 462:64–74.
- [3] Pop CS, Hussien MD, Popa M, Mares A, Grumezescu AM, Grigore R, Lazar V, Chifiriuc MC, Sakizlian M, Bezirtoglou E, Bertesteanu S. Metallic-based micro and nanostructures with antimicrobial activity. *Curr Top Med Chem*, 2015, 15(16): 1577–1582.
- [4] Lansdown AB, Mirastschijski U, Stubbs N, Scanlon E, Agren MS. Zinc in wound healing: theoretical, experimental, and clinical aspects. *Wound Repair Regen*, 2007, 15(1):2–16.
- [5] Agren M.S. Studies on zinc in wound healing. *Acta Derm Venereol Suppl (Stockh)*, 1990, 154:1–36.
- [6] Andersson-Willman B, Gehrmann U, Cansu Z, Buerki-Thurnherr T, Krug HF, Gabrielsson S, Scheynius A. Effects of subtoxic concentrations of TiO₂ and ZnO nanoparticles on human lymphocytes, dendritic cells and exosome production. *Toxicol Appl Pharmacol*, 2012, 264(1):94–103.
- [7] Ilves M, Palomäki J, Vippola M, Lehto M, Savolainen K, Savinko T, Alenius H. Topically applied ZnO nanoparticles suppress allergen induced skin inflammation but induce vigorous IgE production in the atopic dermatitis mouse model. *Part Fibre Toxicol*, 2014, 11:38.
- [8] Agren MS, Franzén L, Chvapil M. Effects on wound healing of zinc oxide in a hydrocolloid dressing. *J Am Acad Dermatol*, 1993, 29(2 Pt 1):221–227.
- [9] Kim HS. Do not put too much value on conventional medicines. *J Ethnopharmacol*, 2005, 100(1–2):37–39.
- [10] Liakos I, Rizzello L, Scurr DJ, Pompa PP, Bayer IS, Athanassiou A. All-natural composite wound dressing films of essential oils encapsulated in sodium alginate with antimicrobial properties. *Int J Pharm*, 2014, 463(2):137–145.
- [11] Oprea AE, Pandel LM, Dumitrescu AM, Andronescu E, Grumezescu V, Chifiriuc MC, Mogoantă L, Bălşeanu TA, Mogoşanu GD, Socol G, Grumezescu AM, Iordache F, Maniu H, Chirea M, Holban AM. Bioactive ZnO coatings deposited by MAPLE – an appropriate strategy to produce efficient anti-biofilm surfaces. *Molecules*, 2016 Feb 26, 21(2).
- [12] Fufă MO, Mihaiescu DE, Mogoantă L, Bălşeanu TA, Mogoşanu GD, Grumezescu AM, Bolcan A. *In vivo* biotransformation of CNTs using a BALB/c mouse experimental model. *Rom J Morphol Embryol*, 2015, 56(4):1481–1493.
- [13] Istrate CM, Holban AM, Grumezescu AM, Mogoantă L, Mogoşanu GD, Savopol T, Moisescu M, Iordache M, Vasile BS, Kovacs E. Iron oxide nanoparticles modulate the interaction of different antibiotics with cellular membranes. *Rom J Morphol Embryol*, 2014, 55(3):849–856.
- [14] Bowler PG. Wound pathophysiology, infection and therapeutic options. *Ann Med*, 2002, 34(6):419–427.
- [15] Ionescu B, Ionescu D, Gheorghe I, Mihaescu G, Bleotu C, Sakizlian M, Banu O. *Staphylococcus aureus* virulence phenotypes among Romanian population. *Biointerface Res Appl Chem*, 2015, 5(3):945–948.
- [16] Vasile BS, Oprea O, Voicu G, Ficai A, Andronescu E, Teodorescu A, Holban A. Synthesis and characterization of a novel controlled release zinc oxide/gentamicin–chitosan composite with potential applications in wounds care. *Int J Pharm*, 2014, 463(2):161–169.
- [17] Pasquet J, Chevalier Y, Couval E, Bouvier D, Bolzinger MA. Zinc oxide as a new antimicrobial preservative of topical products: interactions with common formulation ingredients. *Int J Pharm*, 2015, 479(1):88–95.
- [18] Pasquet J, Chevalier Y, Couval E, Bouvier D, Noizet G, Morlière C, Bolzinger MA. Antimicrobial activity of zinc oxide particles on five micro-organisms of the Challenge Tests related to their physicochemical properties. *Int J Pharm*, 2014, 460(1–2):92–100.
- [19] El Asbahani A, Miladi K, Badri W, Sala M, Aït Addi EH, Casabianca H, El Mousadik A, Hartmann D, Jilale A, Renaud FN, Elaissari A. Essential oils: from extraction to encapsulation. *Int J Pharm*, 2015, 483(1–2):220–243.
- [20] Haba E, Bouhdid S, Torrego-Solana N, Marqués AM, Espuny MJ, García-Celma MJ, Manresa A. Rhamnolipids as emulsifying agents for essential oil formulations: antimicrobial effect against *Candida albicans* and methicillin-resistant *Staphylococcus aureus*. *Int J Pharm*, 2014, 476(1–2): 134–141.
- [21] Anghel I, Holban AM, Andronescu E, Grumezescu AM, Chifiriuc MC. Efficient surface functionalization of wound dressings by a phytoactive nanocoating refractory to *Candida albicans* biofilm development. *Biointerphases*, 2013, 8:12.
- [22] Anghel I, Grumezescu AM, Holban AM, Ficai A, Anghel AG, Chifiriuc MC. Biohybrid nanostructured iron oxide nanoparticles and *Satureja hortensis* to prevent fungal biofilm development. *Int J Mol Sci*, 2013, 14(9):18110–18123.
- [23] Budzyńska A, Sadowska B, Wieckowska-Szakiel M, Różalska B. *In vitro* efficacy analysis of absorbent dressing modified with essential oils, against *Staphylococcus aureus* and *Candida albicans*. *Med Dosw Mikrobiol*, 2013, 65(2):77–86.

- [24] Chin KB, Cordell B. The effect of tea tree oil (*Melaleuca alternifolia*) on wound healing using a dressing model. *J Altern Complement Med*, 2013, 19(12):942–945.
- [25] Bennett DC, Leung G, Wang E, Ma S, Lo BK, McElwee KJ, Cheng KM. Ratite oils promote keratinocyte cell growth and inhibit leukocyte activation. *Poult Sci*, 2015, 94(9):2288–2296.
- [26] Marques JPR, Amorim L, Silva-Junior GJ, Spósito MB, Appezato-da Gloria B. Structural and biochemical characteristics of *Citrus* flowers associated with defense against a fungal pathogen. *AoB Plants*, 2014 Dec 22, 7.
- [27] Najm WA, Bolocan A, Ionescu D, Ionescu B, Gheorghe I, Banu O, Mihailescu D, Decuseara A. Etiology and resistance patterns of *Pseudomonas aeruginosa* strains isolated from a Romanian hospital. *Biointerface Res Appl Chem*, 2015, 5(5):986–991.
- [28] Fufă O, Andronescu E, Grumezescu V, Holban AM, Mogoantă L, Mogoșanu GD, Socol G, Iordache F, Chifiriuc MC, Grumezescu AM. Silver nanostructured surfaces prepared by MAPLE for biofilm prevention. *Biointerface Res Appl Chem*, 2015, 5(6):1011–1017.
- [29] Islan GA, Dini C, Bartel LC, Bolzán AD, Castro GR. Characterization of smart auto-degradative hydrogel matrix containing alginate lyase to enhance levofloxacin delivery against bacterial biofilms. *Int J Pharm*, 2015, 496(2):953–964.
- [30] Palumbo FS, Bavuso Volpe A, Cusimano MG, Pitarresi G, Giammona G, Schillaci D. A polycarboxylic/amino functionalized hyaluronic acid derivative for the production of pH sensible hydrogels in the prevention of bacterial adhesion on biomedical surfaces. *Int J Pharm*, 2015, 478(1):70–77.
- [31] Shenderovich J, Feldman M, Kirmayer D, Al-Quntar A, Steinberg D, Lavy E, Friedman M. Local sustained-release delivery systems of the antibiofilm agent thiazolidinedione-8 for prevention of catheter-associated urinary tract infections. *Int J Pharm*, 2015, 485(1–2):164–170.
- [32] Archer NK, Mazaitis MJ, Costerton JW, Leid JG, Powers ME, Shirtliff ME. *Staphylococcus aureus* biofilms: properties, regulation, and roles in human disease. *Virulence*, 2011, 2(5):445–459.
- [33] Gjødtsbøl K, Christensen JJ, Karlsmark T, Jørgensen B, Klein BM, Krogfelt KA. Multiple bacterial species reside in chronic wounds: a longitudinal study. *Int Wound J*, 2006, 3(3):225–231.
- [34] Schierle CF, De la Garza M, Mustoe TA, Galiano RD. Staphylococcal biofilms impair wound healing by delaying reepithelialization in a murine cutaneous wound model. *Wound Repair Regen*, 2009, 17(3):354–359.
- [35] Cristea AD, Popa M, Chirifiuc MC, Marutescu L, Lazar V, Suciu I, Iliescu A, Dimitriu B, Perlea P. The antimicrobial efficiency of endodontic irrigation solutions on bacterial biofilm. A literature review. *Biointerface Res Appl Chem*, 2015, 5(4):963–969.

Corresponding author

Alexandru Mihai Grumezescu, Chem Eng, PhD, Department of Science and Engineering of Oxide Materials and Nanomaterials, Faculty of Applied Chemistry and Materials Science, Politehnica University of Bucharest, 1–7 Polizu Street, 011061 Bucharest, Romania; Phone +4021–402 39 97, e-mail: grumezescu@yahoo.com

Received: March 31, 2016

Accepted: May 2, 2016